sustainability

MDPI

Article

Analysis of Ecological Environmental Quality Change in the Yellow River Basin Using the Remote-Sensing-Based Ecological Index

Zekang Yang, Jia Tian *, Wenrui Su, Jingjing Wu, Jie Liu, Wenjuan Liu and Ruiyan Guo

School of Agriculture, Ningxia University, Yinchuan 750021, China
* Correspondence: tianjia@nxu.edu.cn

Abstract: Establishing a method for characterizing spatiotemporal changes in the quality of the ecological environment in a timely and accurate manner is of great significance for the protection and sustainable development of the ecological environment in the Yellow River Basin (YRB). In this study, the Google Earth Engine (GEE) platform was used as a basis for constructing the remote-sensing-based ecological index (RSEI), and the RSEI was used to evaluate the quality of the ecological environment in the YRB. The results indicated that the mean of the RSEI values showed two stages of rapid improvement and slow improvement during 1990–2020. From 1990 to 2000, the average growth trend was 0.005/a with a growth rate of 21.15%, with the main contributions of bad to poor (101,800 km^2), poor to medium (56,900 km^2), and medium to good (70,800 km^2) ecological environmental quality levels. From 2000 to 2020, the average growth trend was 0.002/a with a growth rate of 2.13%, with main contributions of poor to bad (65,100 km^2) and good to medium (35,200 km^2) ecological environmental quality levels. From 1990 to 2020, there was a 76.38% improvement in the ecological environmental quality of the entire YRB, in which significant improvement accounted for 26.14%. The reductions in the ecological environmental quality accounted for 23.62%, of which significant reductions accounted for just 1.46%. The improvement in the ecological environmental quality of the YRB showed a trend of increasing sustainability, which is expected to continue. The distribution of the ecological environmental quality in the YRB showed obvious regional aggregation, whereby cold spots were concentrated in the northern and central regions of the YRB, which are the sandy and hilly ravine areas of the Loess Plateau. However, the areas corresponding to hot spot clusters decreased with time, and their significance also decreased. Thus, our study demonstrates that the GEE platform can be used to determine the spatiotemporal changes in the ecological environmental quality of the YRB in a timely and accurate manner.

Keywords: remote-sensing-based ecological index; ecological environmental quality; google earth engine; yellow river basin

Citation: Yang, Z.; Tian, J.; Su, W.; Wu, J.; Liu, J.; Liu, W.; Guo, R. Analysis of Ecological Environmental Quality Change in the Yellow River Basin Using the Remote-Sensing-Based Ecological Index. *Sustainability* **2022**, *14*, 10726. https://doi.org/10.3390/su141710726

Academic Editors: Jiankun Huang, Yunqi Wang, Liqun Lyu and Jun Li

Received: 27 June 2022
Accepted: 24 August 2022
Published: 29 August 2022

1. Introduction

The YRB plays an important role in China's economic and social development and ecological security. It is an important ecological function area in China and a key area of concern for the various parties and the government. In his speech on September 18, General Secretary Xi Jinping identified ecological protection and high-quality development in the YRB as a major national strategy [1]. However, the YRB is also an area with a very fragile ecological environment, with the most serious soil erosion in China [2]. Floods, landslides and other disasters occur frequently. For this reason, China has successfully implemented and managed the "Three-North Shelter Forest Project" and "Returning Farmland to Forest and Grass Project" in the YRB since 1978. A series of major ecological forestry projects have greatly improved the ecological environment in this area [3]. Although the overall ecological environment of the YRB is improving, there are still some areas where

the ecological environment is deteriorating due to the influence of human production activities [4]. As the social and economic development of the YRB shifts from having a high growth rate to having high-quality growth, long-term remote sensing monitoring of the regional ecological environmental quality has become an important means to quantitatively evaluate the ecological environment and its change trends, which is an important basis for development [5]. Although researchers have proposed a variety of ecological environmental quality evaluation indicators, there are generally problems encountered during the actual monitoring, such as difficulties with index extraction, inadequately small research scales, and slow data updates [6]. Therefore, a suitable method for characterizing the spatiotemporal changes in the ecological environmental quality of the YRB in a timely and accurate manner must be established to ensure the protection of the ecological environment and the sustainable development of the YRB.

Due to the advantages of allowing rapid, real-time, and large-scale evaluations [7,8], satellite remote sensing has become the main means of evaluating the quality of regional ecological environments [9]. However, most studies have used remote sensing information to extract only a single index for this evaluation. For example, Ivits et al. [10] evaluated the suitability of farmland bird habitats according to the normalized vegetation index (NDVI), Coutts et al. [11] evaluated the urban heat island effect using the land surface thermal temperature (LST), and Guo et al. [12] used the water body index (NDWI) to extract water body information. However, an ecological environment is a combination of multiple factors. Although evaluations based on a single index have certain value, it is difficult to explain the comprehensive effects of multiple factors in an ecological environment [10–13]. The remote-sensing-based ecological index (RSEI) based on Landsat, proposed by Xu [14] in 2013, provides a new direction for the evaluation of ecological environmental quality. Since the RSEI integrates the four ecological indicators of greenness (NDVI), humidity (Wet), heat (LST), and dryness (NDSI), and as the indicators are easy to obtain, there is no need to manually set the weights, which are instead determined via a principal component analysis; therefore, the RSEI can comprehensively, quickly, and objectively reflect the regional ecological environmental quality level. At present, the RSEI has been widely used in the evaluation of regional ecological environmental quality [15–18]; however, applying it to a large regional scale, such as the entire YRB, requires a huge amount of data, resulting in significant complexity in data preprocessing and an exponential increase in the associated required computational work [19]. In order to solve this problem, Wang et al. [6] and Chen et al. [9] combined the Google Earth Engine (GEE) remote sensing cloud platform with the RSEI to evaluate the quality of the ecological environment of the Guangdong–Hong Kong–Macao Greater Bay Area urban agglomeration, and they assessed the ecological environment of the Sanjiangyuan area through dynamic monitoring and an analysis of the environmental quality. The results showed that GEE, as a remote sensing computing platform for the evaluation and monitoring of ecological environmental quality in a large area, can address the problems of missing remote sensing data, color differences, and time inconsistencies [20]. Furthermore, it can avoid complicated data preprocessing steps such as radiation correction, atmospheric correction, and orthophoto correction [21], and other types of processing approaches such as image cloud removal, mosaic, index calculation, statistics, and dynamic change trend analysis methods can be quickly realized [22]. In recent decades, many researchers of the YRB have conducted in-depth studies on climate changes [23], land-use pattern evolution [24], water area changes [25], air quality [26], and water pollution [27], assessing the relationship between disasters and the ecological environment quality of the YRB. As the ecological environment has improved, disasters have been in relative decline. However, most previous studies were carried out by considering a single element or specific areas, such as the upper, middle, or lower reaches of the Yellow River; hence, they cannot comprehensively and holistically represent the ecological environmental quality of the entire YRB.

Therefore, this paper used the GEE platform, taking the entire YRB as the research area; used Landsat remote sensing images as the data source; and performed image

preprocessing and synthesis steps for the calculation of the remote-sensing-based ecological index (RSEI) in the GEE cloud. Using the calculation results to analyze and evaluate the spatiotemporal changes in the ecological environmental quality of the YRB on a large scale and over a long-term time series, this study can provide a theoretical basis and technical support for the ecological environment protection and high-quality development and disaster prevention of the YRB.

2. Study Area

The YRB is located in the central and northern parts of China (E: 95°53′–119°05′, N: 32°10′–41°50′), and the basin spans Qinghai, Sichuan, Gansu, Ningxia, Inner Mongolia, Shaanxi, Shanxi, Henan, and nine provinces in Shandong (Figure 1), with a total area of about 800,000 km^2 [4]. The basin presents arid, semi-arid, semi-humid, and humid climates from west to east. The annual average temperature is around 7 °C, and the average precipitation is around 440 mm [28]. The spatial distributions of precipitation and temperature show a trend of decreasing from both east to west and south to north. The terrain of the basin is high in the west and low in the east, spanning the Qinghai–Tibet Plateau, Inner Mongolia Plateau, Loess Plateau, and Huaihai Plain from west to east. Due to the large climatic differences and complex geomorphological units, the YRB has become one of the most vulnerable areas in the country's ecological environment, mainly manifesting as the gradual reduction in runoff, serious water pollution, intensified soil erosion, land desertification, and vegetation degradation [29].

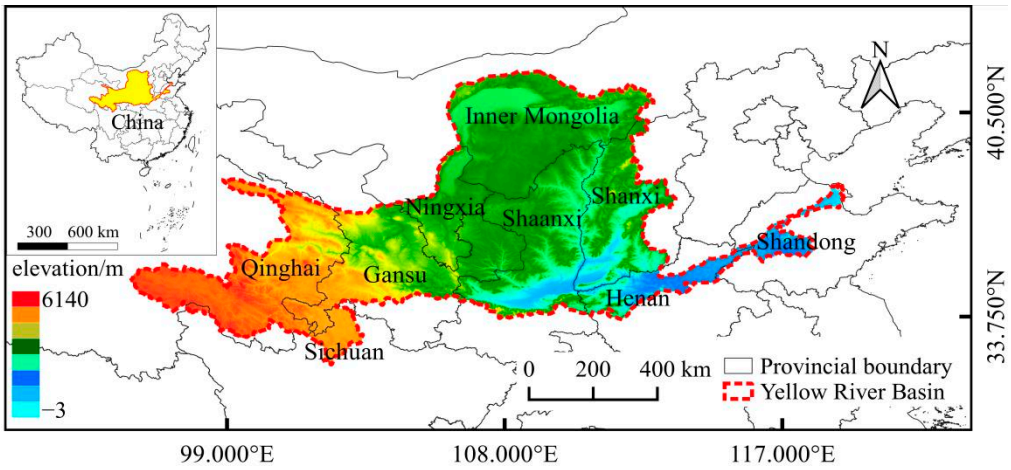

Figure 1. Map of the study area.

3. Materials and Methods

3.1. Data and Preconditioning

The remote sensing images came directly from the T1-level (highest quality) Landsat 5 (TM) and Landsat 8 (OLI) surface reflectance data products (surface reflectance, SR) provided by the GEE platform database, and they were geometrically and radiometrically corrected, along with atmospheric correction, with a spatial resolution of 30 m and a temporal resolution of 16 days. Through GEE programming (JavaScript), the screening imaging time was set as the target year and summer (June–September) remote sensing images for 1 year before and after the target year. The numbers of images were 931 (1990), 921 (1995), 1128 (2000), 1132 (2005), 1078 (2010), 1409 (2015), 1287 (2020), with a total of 7886 (Figure 2). On the GEE platform, the officially provided Landsat cloud mask algorithm was used to remove cloud pixels from the input image dataset conforming to the time and space range, and the minimum cloud amount image from the summer of the target year was synthesized with the median value of the cloud-free pixels. In addition, in order for the humidity index to accurately represent the humidity conditions of the ground and

avoid large areas of water affecting the load distribution of the principal components, the MNDWI water body index was used to mask water body information [14].

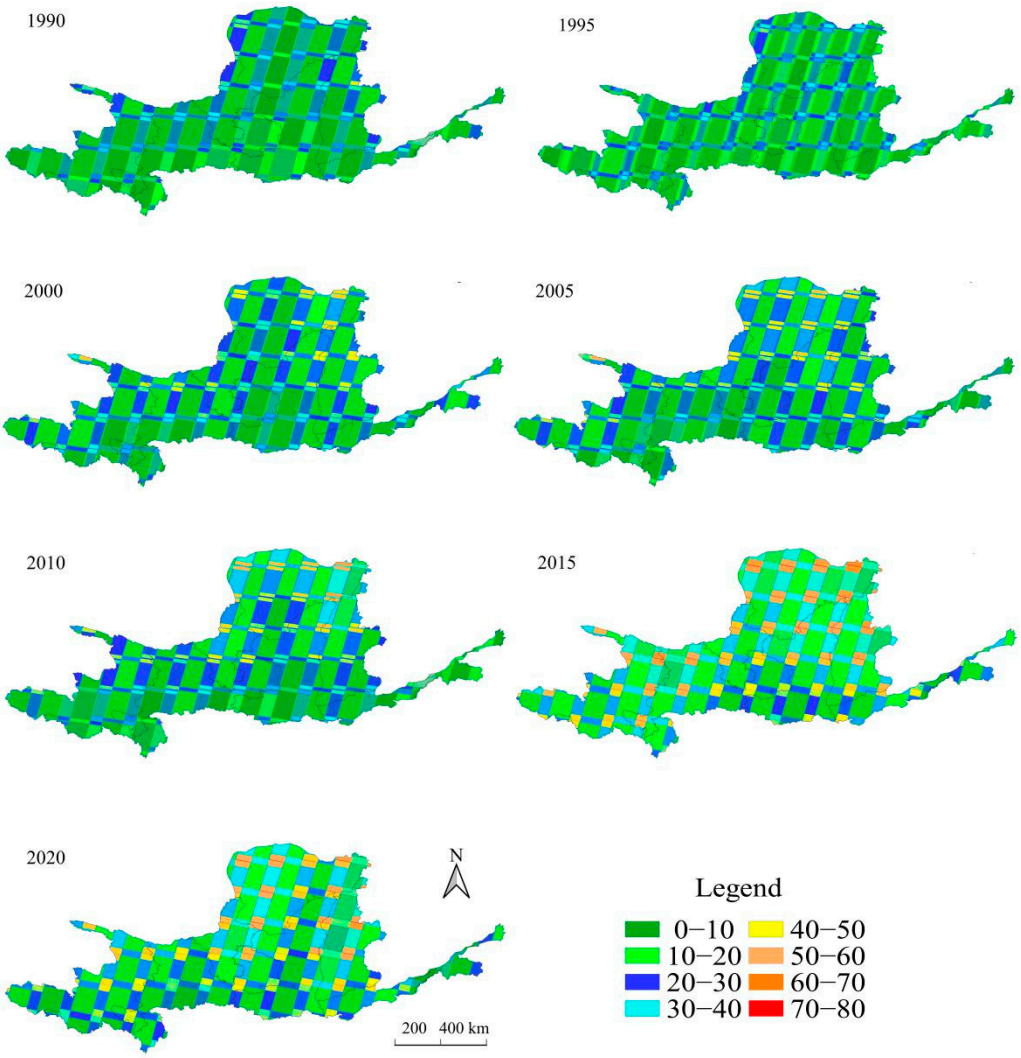

Figure 2. Landsat images used to produce clear imagery.

3.2. Calculation of the Remote-Sensing-Based Ecological Index (RSEI)

To comprehensively reflect the ecological environmental quality of the region, the remote-sensing-based ecological index (RSEI) was constructed based on four selected indicators, greenness (NDVI), humidity (Wet), heat (LST), and dryness (NDSI), and the calculation formula is shown in Table 1. Since their dimensions are not uniform, forward normalization (MMS) was performed on these four indicators prior to principal component analysis (PCA), and their values were mapped according to the (0, 1) interval, as shown in Equation (1).

$$MMS = (I - I_{min})/(I_{max} - I_{min}) \quad (1)$$

Here, I is the indicator value, I_{max} is the maximum value of the indicator in the target year, and I_{min} is the minimum value of the indicator in the target year. After MMS processing, the four indicators were synthesized into a new image, and the initial $RSEI_0$ (unnormalized) was calculated by writing a principal component analysis script (PCA JavaScript) in GEE, as shown in Equation (2).

$$RSEI_0 = PC1[f\ (Wet, NDVI, NDSI, LST)] \quad (2)$$

Table 1. Methods used for calculation of the indicators.

Indicators	Calculation Method
NDVI	$NDVI = (\rho_{NIR} - \rho_{red})/(\rho_{NIR} + \rho_{red})$
Wet	$Wet_{TM} = 0.0315\rho_{blue} + 0.2021\rho_{green} + 0.3102\rho_{red} + 0.1594\rho_{NIR} - 0.6806\rho_{SWIR1} - 0.6109\rho_{SWIR2}$ $Wet_{OLI} = 0.1511\rho_{blue} + 0.1973\rho_{green} + 0.3283\rho_{red} + 0.3407\rho_{NIR} - 0.7117\rho_{SWIR1} - 0.4559\rho_{SWIR2}$
LST	$LST = T/[1 + (\lambda T/\rho)\ln\varepsilon] - 273.15$
NDSI	$NDSI = (SI + IBI)/2$ $IBI = IBI_1/IBI_2$ $IBI_1 = 2\rho_{SWIR2}/(\rho_{SWIR1} + \rho_{NIR}) - [(\rho_{NIR}/(\rho_{red} + \rho_{NIR}) + \rho_{green}/(\rho_{SWIR1} + \rho_{green})]$ $IBI_2 = 2\rho_{SWIR2}/(\rho_{SWIR1} + \rho_{NIR}) + [(\rho_{NIR}/(\rho_{red} + \rho_{NIR}) + \rho_{green}/(\rho_{SWIR1} + \rho_{green})]$ $SI = [(\rho_{SWIR1} + \rho_{red}) - (\rho_{blue} + \rho_{NIR})]/[(\rho_{SWIR1} + \rho_{red}) + (\rho_{blue} + \rho_{NIR})]$

Note: T is the heat value at the sensor, λ is the central wavelength of the thermal infrared band, ρ is a constant, and ε is the surface-specific emissivity. All parameter values refer to [30].

Here, PC1 is the first principal component and f is the forward normalization processing (MMS) for the four indicators, which also uses Equation (1) to perform MMS processing on RSEI0 to obtain the final RSEI value, as shown in Equation (3). Its value is in the range (0, 1), and an RSEI value closer to 1 indicates the better quality of the ecological environment.

$$RSEI = (RESI_0 - RSEI_{0min})/(RESI_{0max} - RSEI_{0min}) \quad (3)$$

Here, $RSEI_{0min}$ and $RESI_{0max}$ are the minimum and maximum values of $RESI_0$ in the target year, respectively, and RSEI is the final remote-sensing-based ecological index. The RSEI can be divided into five levels with intervals of 0.2, I (0–0.2), II (0.2–0.4), III (0.4–0.6), IV (0.6–0.8), and V (0.8–1.0), which represent the quality of the ecological environment. The five levels indicate bad, poor, medium, good, and excellent quality, respectively [14,31]. The technical flowchart of this paper is shown in Figure 3.

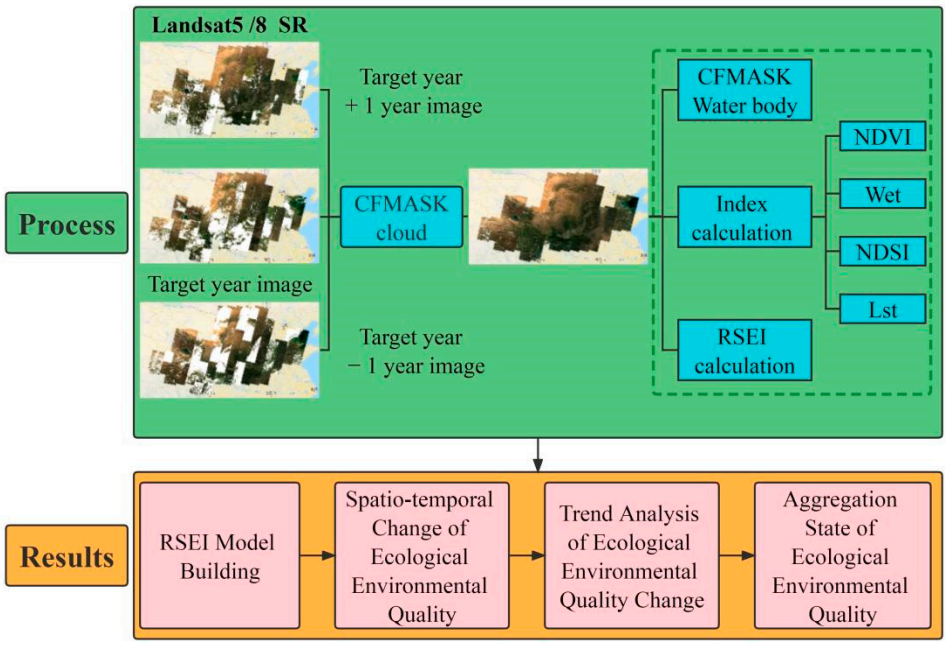

Figure 3. Flowchart for analysis of the ecological environmental quality changes in the YRB.

4. Results

4.1. RSEI Model Building

It can be seen from Table 2 that the loads of greenness (NDVI) and humidity (Wet) in the four indicators were positive, and the average load of the greenness (0.6624) was

greater than that of humidity (0.4112), indicating that the contribution of the greenness to the RSEI was higher than that of the humidity. The loads of heat (LST) and dryness (NDSI) were negative, and the absolute value of the average load of the heat (0.2499) was smaller than that of the dryness (0.5547), indicating that the contribution of the heat to the RSEI was lower than that of the dryness. This is consistent with the actual situation. In addition, the contribution rate of the four indicators to the first principal component (PC1) reached 93.87% (2000) at the highest and 87.43% (1990) at the lowest, with an average of 89.66%. More than 85% of the characteristic information of each indicator was concentrated on PC1, indicating that it was feasible to construct the RSEI on the basis of PC1 in the YRB. The average correlation model was further used to test the feasibility of the RSEI. The calculation method is shown in Equation (4).

$$\overline{C_p} = \frac{|C_q| + |C_r| + \cdots |C_s|}{n-1} \quad (4)$$

Table 2. Contributions and loadings of four indices to the first principal component (PC1).

PC1					
Year	**NDVI**	**Wet**	**LST**	**NDSI**	**Contribution (%)**
1990	0.6490	0.4121	−0.2754	−0.5772	87.43
1995	0.6544	0.4959	−0.1590	−0.5482	87.79
2000	0.7487	0.4021	−0.0197	−0.5267	93.87
2005	0.6846	0.3623	−0.2572	−0.5779	88.59
2010	0.7248	0.3276	−0.3278	−0.5079	88.57
2015	0.6255	0.4167	−0.2802	−0.5971	90.60
2020	0.5495	0.4619	−0.4297	−0.5477	90.77
Mean	0.6624	0.4112	−0.2499	−0.5547	89.66

Here, $\overline{C}$ is the average correlation degree; p, q, r, and s are the indicators for the correlation analysis; n is the number of indicators for the correlation analysis; and C_p, C_q, C_r, and C_s are the correlation coefficients (Spearman correlation coefficients) between the indicators. The results are shown in Table 3. The average correlation of the RSEI was the largest (0.497), followed by the NDSI (0.406), NDVI (0.356), LST (0.274), and Wet (0.242).

Table 3. Correlation matrix of the indices.

Year	Indicator	NDVI	Wet	LST	NDSI	RSEI
1990–2020	NDVI	1	−0.323	−0.321	−0.423	0.621
	Wet	−0.323	1	0.054	−0.348	0.056
	LST	−0.321	0.054	1	0.447	−0.561
	NDSI	−0.423	−0.348	0.447	1	−0.748
	$\overline{C}$	0.356	0.242	0.274	0.406	0.497

4.2. Spatiotemporal Changes of the Ecological Environmental Quality

Figure 4 shows the mean and distribution of the RSEI over 7 selected years spanning from 1990 to 2020. The results indicate that the overall quality of the ecological environment in the YRB is improving. The mean RSEI increased from 0.4278 in 1990 to 0.4944 in 2020, with an average growth trend of 0.002/a, and a 30 year growth rate of 15.56%. The mean RSEI peaked in 2000 (0.5183), and the lowest value appeared in 1990 (0.4278). At the same time, it can be seen from Figure 5 that the quality of the ecological environment in the YRB increased rapidly during the period from 1990 to 2000, with an average growth trend of 0.005/a and a growth rate of 21.15%. Down → up → down → up fluctuations could be observed, but the overall growth was slow, the average growth trend was 0.002/a, and the growth rate was only 2.13%. Therefore, the changes in the ecological environmental

quality of the YRB can be divided into two stages: before 2000 (1990–2000) and after 2000 (2000–2020).

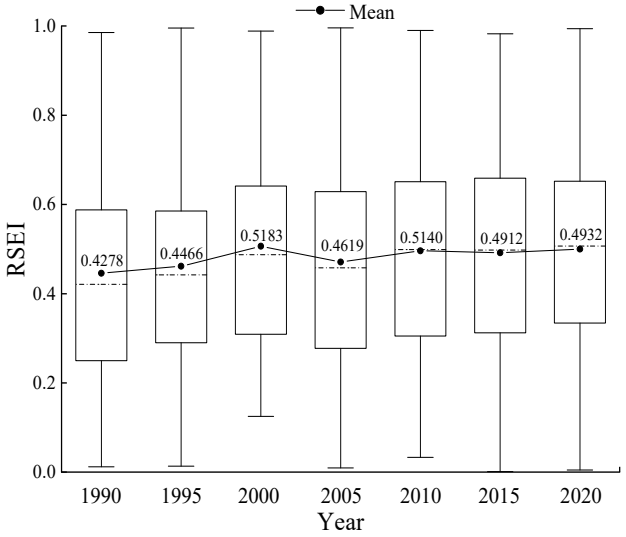

Figure 4. Average and distribution of the RSEI in the YRB, 1990–2020.

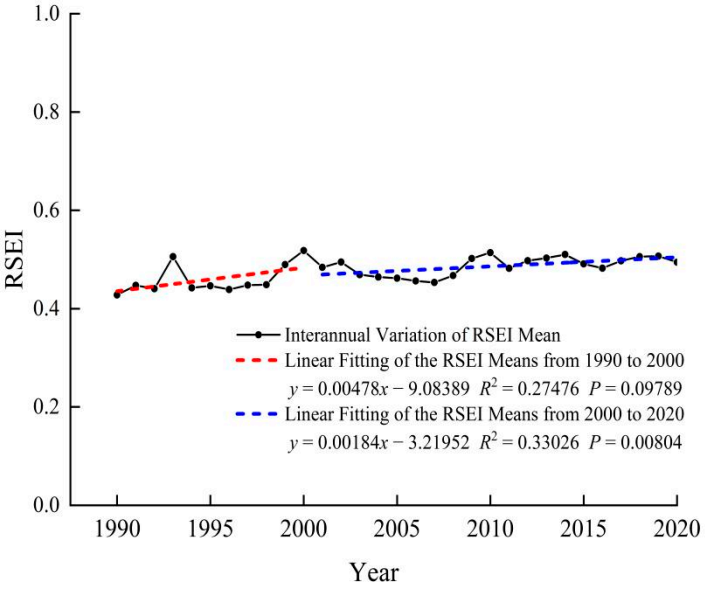

Figure 5. Cross-annual mean variation of the RSEI in the YRB, 1990–2020.

Figure 6 reflects the spatial distribution of RSEI values in the YRB (1990–2020). On the whole, the areas with bad (I) and poor (II) ecological environmental quality were concentrated in the upper and middle reaches of the Yellow River, including the Loess hills in northern Shaanxi and Longzhong, the arid belt in central Ningxia, the Mu Us Sandy Land, and the Kubuqi Desert, among other areas. The ecological environmental quality levels of medium (III) and good (IV) areas were concentrated in the source and downstream of the Yellow River, including southern Gansu, the Qilian Mountains, northern Henan, and northwestern Shandong, as well as irrigation areas (such as Hetao Plain), wetlands (such as Wuliangsuhai), and areas around the forests. The areas with excellent ecological environmental quality (V) were concentrated in national nature reserves, such as the northern foot of the Qinling Mountains, the Liupan the Mountains, Ziwuling Mountains, and the Luliang Mountains.

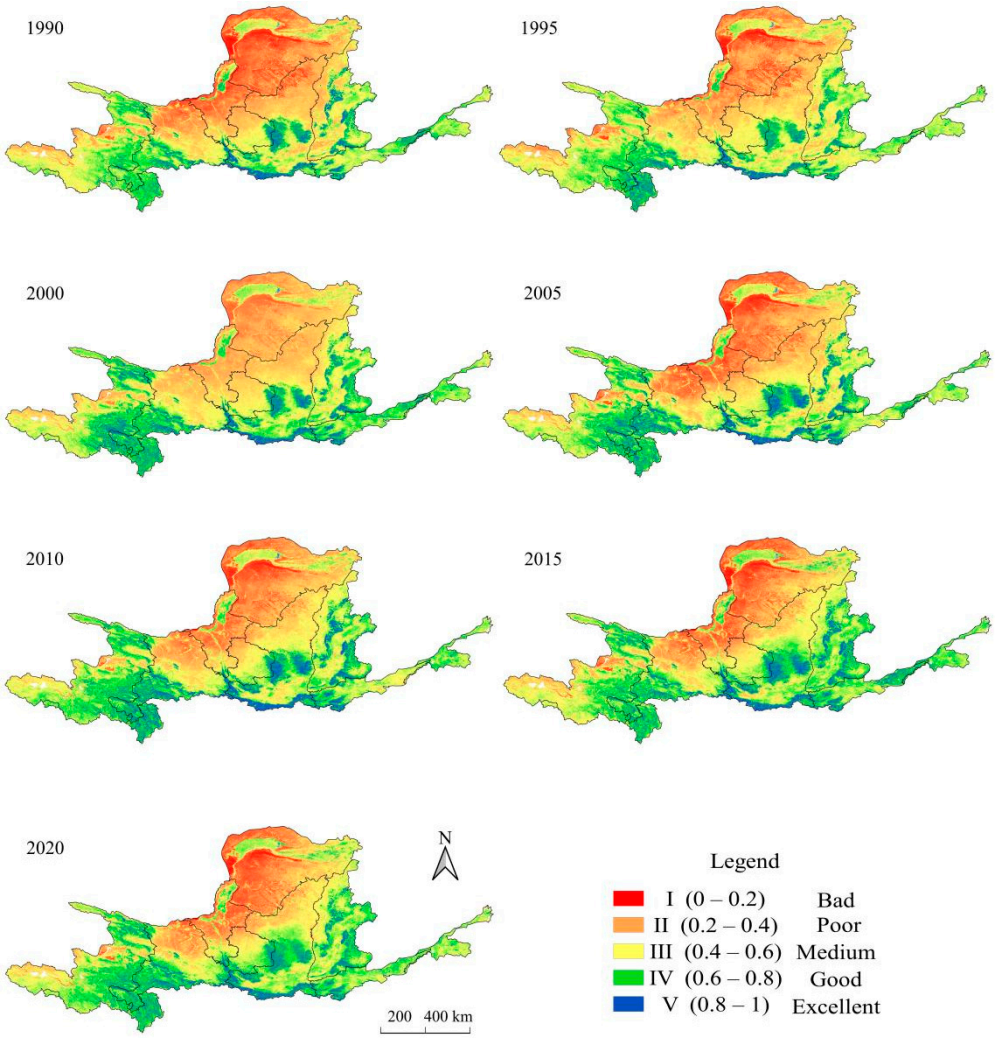

Figure 6. Distribution of the ecological environmental quality levels in the YRB, 1990–2020.

According to Figure 7 (the years from the inner ring to the outer ring are 1990, 1995, 2000, 2005, 2010, 2015, and 2020), the proportion of the area in the YRB with excellent ecological environmental quality increased from 4.99% in 1990 to 8.05% in 2020, corresponding to a growth rate of 61.32%; the proportion of the area with good ecological environmental quality increased from 18.98% in 1990 to 29.21% in 2020, corresponding to a growth rate of 53.90%; the proportion of the area with medium ecological environmental quality increased from 28.67% in 1990 to 31.91% of the total area in 2020, corresponding to a growth rate of 11.30%; the proportion of the area with poor ecological environmental quality decreased from 30.53% in 1990 to 20.77% in 2020, corresponding to a growth rate of −31.97%; the proportion of the area with bad ecological environmental quality decreased from 16.83% in 1990 to 10.06% in 2020, corresponding to a growth rate of −40.23%. From 1990 to 2020, the ecological environmental quality of the YRB showed a trend of continuous improvement. Changes in the proportion of ecological environmental quality in the upper, middle, and lower reaches of the YRB were analyzed (Figure 8). The ecological environmental quality level in the upper and middle reaches of the YRB is in accordance with the overall change trend, while the change trend of the ecological environmental quality level in the lower YRB is completely different. The proportion of the area in the lower YRB with excellent and good levels showed an overall downward trend, while the proportion of the area with bad and poor levels showed an overall upward trend. This is in line with the geographical

location of the lower reaches of the YRB, the process of economic development and urban construction expansion, and government policies.

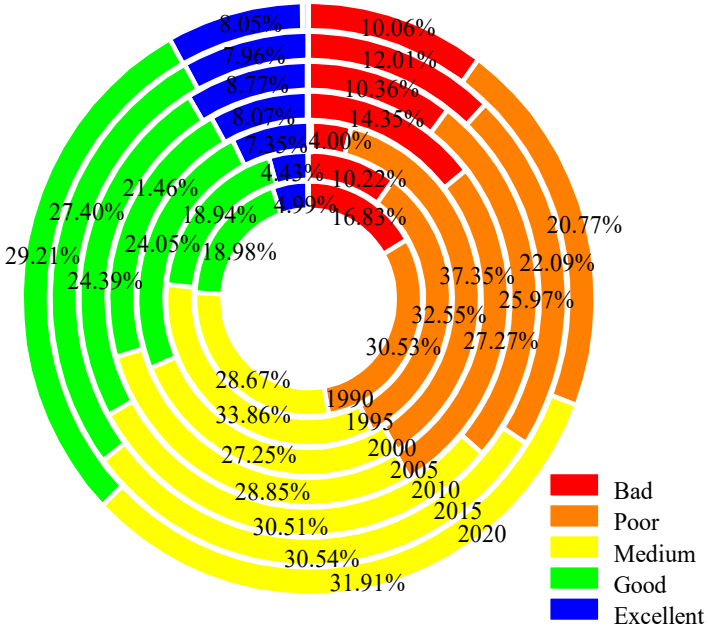

Figure 7. The different levels of ecological environmental quality in the YRB and their proportions, 1990–2020.

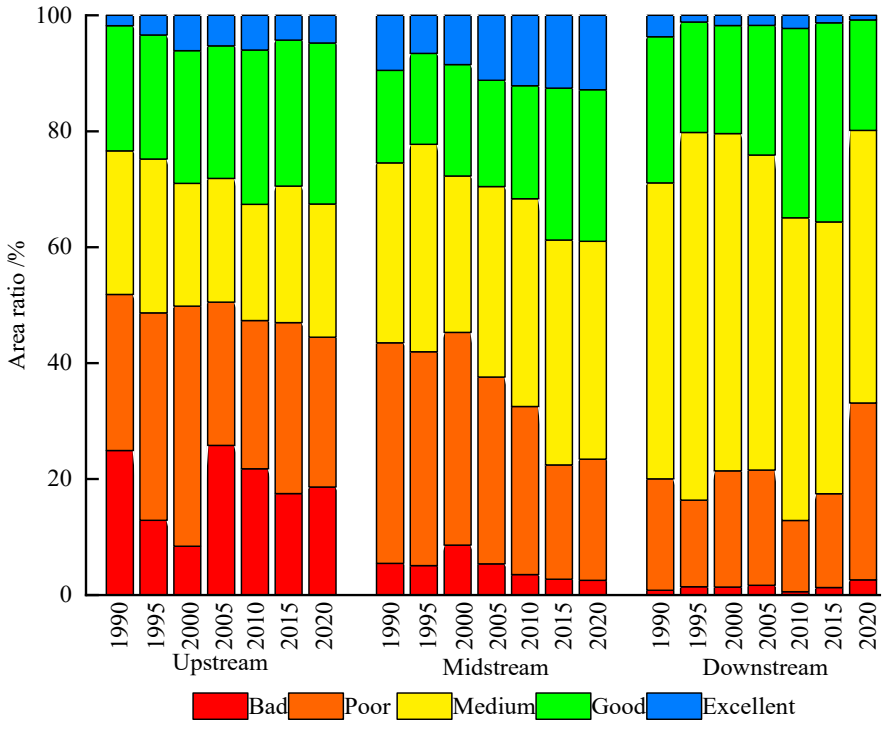

Figure 8. The different levels of ecological environmental quality in the upper, middle, and lower streams of the YRB and their proportions, 1990–2020.

4.3. Trend Analysis of the Ecological Environmental Quality Change

4.3.1. Change of the Ecological Environmental Quality Levels

According to the above analysis, the level of change in the ecological environmental quality of the YRB was studied in two periods (1990–2000 and 2000–2020). It can be seen from Tables 4 and 5 that the ecological environmental quality of the YRB showed a change trend of rapidly improving to slowly improving from 1990 to 2020. The specific analysis is presented below.

Table 4. Transition matrix of the ecological environmental quality levels in the YRB, 1990–2000.

Ecological Environmental Quality Levels		2000				
		Bad (I)	**Poor (II)**	**Medium (III)**	**Good (IV)**	**Excellent (V)**
1990	Bad (I)	31,135	101,846	492	30	
	Poor (II)	232	187,745	56,922	1543	22
	Medium (III)	9	11,766	146,659	70,846	1424
	Good (IV)		66	14,110	114,290	24,285
	Excellent (V)			57	6709	33,328

Table 5. Transition matrix of the ecological environmental quality levels in the YRB, 2000–2020.

Ecological Environmental Quality Levels.		2020				
		Bad (I)	**Poor (II)**	**Medium (III)**	**Good (IV)**	**Excellent (V)**
2000	Bad (I)	28,248	2832	239	24	1
	Poor (II)	65,079	155,281	76,982	4042	24
	Medium (III)	12	13,375	134,174	69,964	683
	Good (IV)	4	1030	35,228	142,718	14,450
	Excellent (V)		14	351	19,806	38,891

During the period from 1990 to 2000, it can be seen from Table 4 that the area with an improved ecological environmental quality level was 257,400 km^2, accounting for 32.04% of the total area of the YRB, while the area with a degraded ecological environmental quality level was 32,900 km^2, accounting for 4.10% of the total area of the YRB. The area that improved was 27.94% greater than the degraded area, which indicates that the quality of the ecological environment rapidly improved during this period. It can also be seen from Table 4 that the rapid improvement of the ecological environmental quality was mainly due to the changes from bad to poor (101,800 km^2), from poor to medium (56,900 km^2), and from medium to good (70,800 km^2).

From 2000 to 2020, it can be seen from Table 5 that the area with an improved ecological environmental quality level was 169,200 km^2, accounting for 21.06% of the total area of the YRB, while the area with a degraded ecological environmental quality level was 134,900 km^2, which accounted for 16.79% of the total area of the YRB. The improved area was only 4.27% more than the degraded area, which shows that the quality of the ecological environment improved slowly during this period. It can also be seen from Table 5 that the slow improvement of the ecological environmental quality was mainly due to the large contribution of changes from poor to bad (65,100 km^2) and good to medium (35,200 km^2).

4.3.2. Change Trend and Significance of the Ecological Environmental Quality

The ridge regression function officially provided by GEE was used to fit the RSEI variation trend of the YRB from 1990 to 2020, and the corresponding significance (p-value) was obtained. Figure 9 shows that the ecological environmental quality rapidly deteriorated in key national development zones such as the Ningxia Yanhuang Economic Zone, the Guanzhong–Tianshui Economic Zone, the Hubaoeyu Economic Zone, and

the Central Plains Economic Zone. In Shaanxi Yulin, Yan'an, Ningxia Guyuan, Gansu Pingliang, and other mountainous and hilly areas, the quality of the ecological environment recovered rapidly.

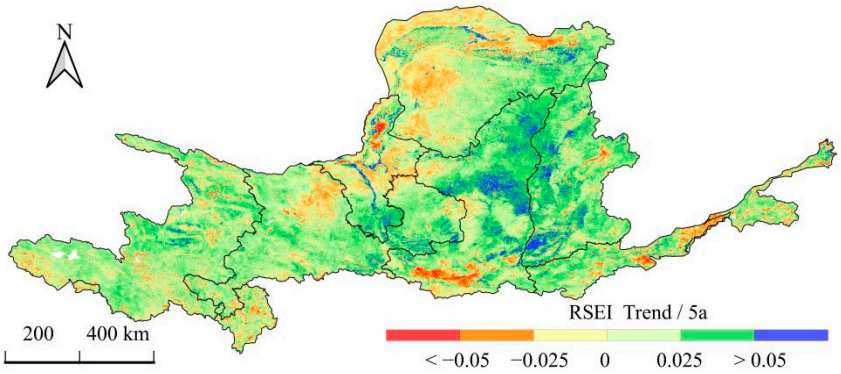

Figure 9. Trends of the RSEI in the YRB, 1990–2020.

As shown in Figure 10, the change trend of ecological environmental quality was divided into four levels: significantly increased ($p < 0.05$), increased but not significant ($p > 0.05$), significantly decreased ($p < 0.05$), and decreased but not significant ($p > 0.05$). According to the relevant statistics (Figure 10), the area with improved ecological environmental quality accounted for 76.38% of the total area of the YRB, of which the area with significant improvement accounted for 26.14%. The area with reduced ecological environmental quality accounted for 23.62% of the total area of the YRB, of which only 1.46% was significantly reduced. The area in which the ecological environmental quality of the YRB improved was 52.76% more than the area in which quality decreased, showing an overall upward trend.

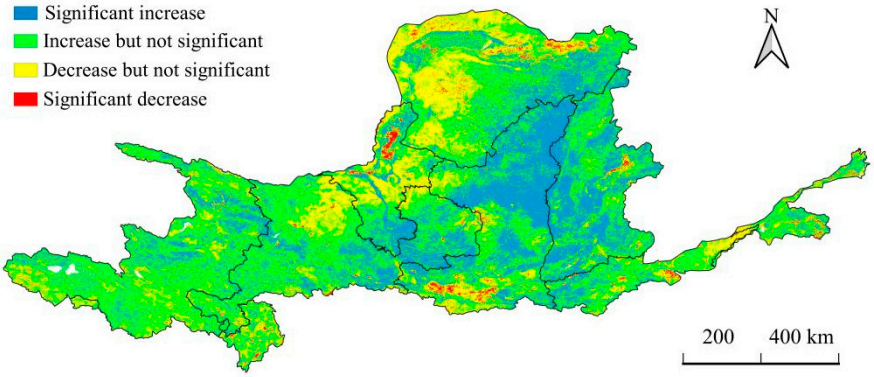

Figure 10. Significance of the RSEI trends.

4.3.3. Sustainability Analysis

The Hurst index is widely used to evaluate time series trend changes [32]. A pixel-by-pixel Hurst index analysis of the RSEI in the YRB from 1990 to 2020 was carried out, and the results are shown in Figure 11. The average Hurst index of RSEI in the YRB was 0.9175. Specifically, the number of pixels with $H < 0.5$ only accounted for 0.12%, revealing weak anti-sustainability ($0.25 \leq H < 0.5$). The number of pixels with $H \geq 0.5$ accounted for 99.88%. Specifically, only 8.78% of the pixels with $H \geq 0.5$ showed weak sustainability ($0.5 < H \leq 0.75$), while the remaining 91.09% of the pixels showed strong sustainability ($0.75 < H \leq 1$). It can also be seen from Figure 11 that the areas with strong sustainability are mainly distributed in the south of the Hetao Plain, the Taihang Mountains, the Qinling Mountains, the Jinghe River, and most of the Weihe River Basin. The comprehensive

analysis showed that the future change trend of RSEI in the YRB was basically the same as that from 1990 to 2020, with strong continuity, and the ecological environment of the YRB is expected to maintain a trend of continuous improvement in the future.

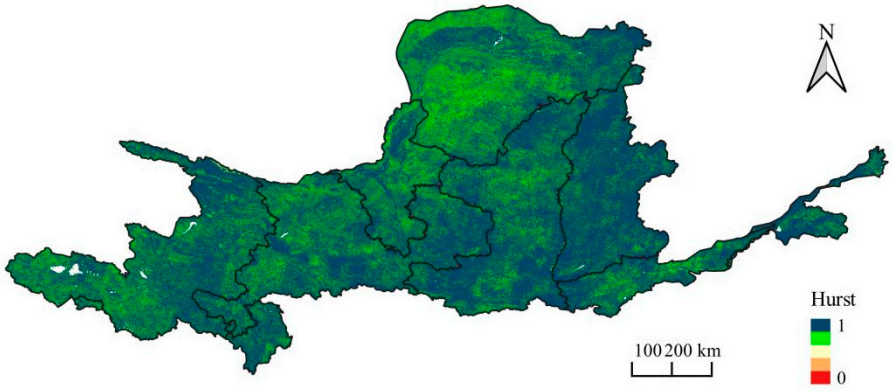

Figure 11. Sustainability of ecological environmental quality in the YRB from 1990 to 2020.

4.4. Aggregation State of the Ecological Environmental Quality

GeoDa software (https://geodacenter.github.io/download.html, accessed on 2 June 2022) was used to generate the global Moran's index for the RSEI of the YRB from 1990 to 2020 (Table 6) [33]. The obtained spatial global autocorrelation coefficients were all positive, with an average value of 0.488, and the spatial correlation was high, which indicates that the spatial distribution of the ecological environmental quality in the YRB was nonrandom and had significant spatial agglomeration distribution characteristics. Areas with good ecological environmental quality were clustered with others of good ecological environmental quality, and areas with poor ecological environmental quality clustered together.

Table 6. The analysis of the spatial autocorrelation of the ecological environmental quality.

Year	Moran's I	*p*	Z
1990	0.453	0.001	5.921
1995	0.418	0.001	5.254
2000	0.526	0.001	6.735
2005	0.538	0.001	6.727
2010	0.519	0.001	6.535
2015	0.483	0.001	6.077
2020	0.480	0.001	6.129
Mean	0.488	0.001	6.197

The remote-sensing-based ecological index values of 76 cities in the YRB were obtained, and a spatial local autocorrelation of ecological environmental quality was also performed through the analysis of hot and cold spots. As shown in Figure 12, as a whole, the distribution of cold and hot spots in the YRB showed obvious regional aggregation, and the cold spots were concentrated in the northern and central urban areas of the YRB, across a wide area, including sandy desert areas and hilly gully areas of the Loess Plateau. The hot spots were concentrated in the Bayankala Mountains and Animaqing Mountains, the upper reaches of the YRB, the Guanzhong Basin, the middle reaches of the YRB, and some urban areas in the lower reaches of the YRB.

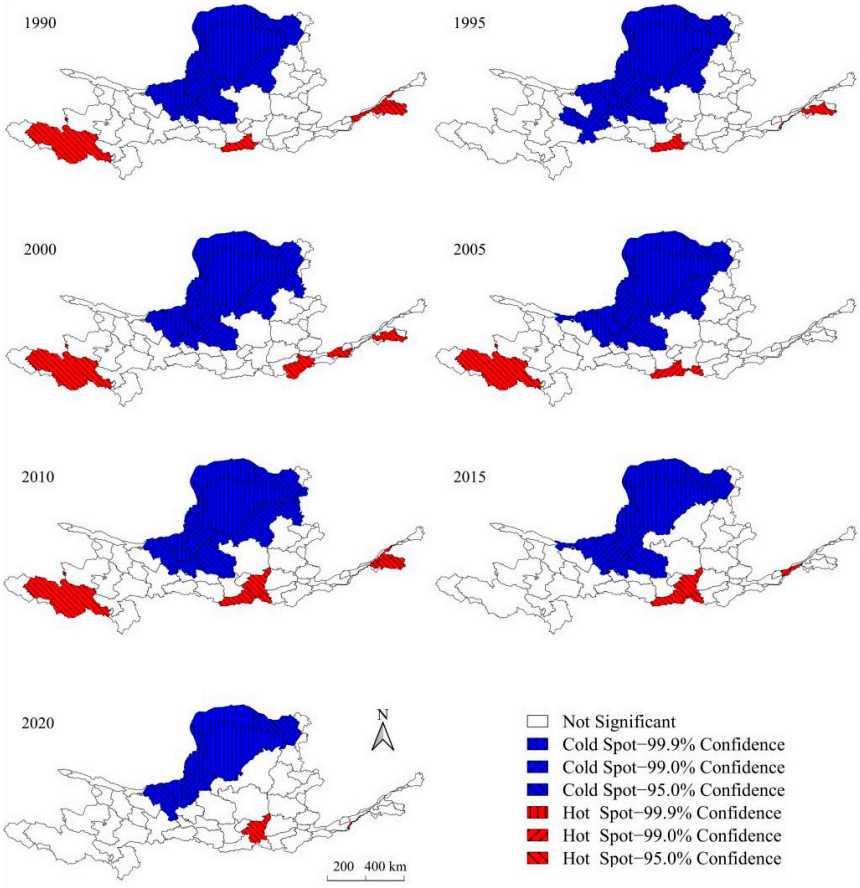

Figure 12. Map of the cold and hot spots (aggregation states) of the ecological environmental quality in the YRB, 1990–2020.

5. Discussion

5.1. Advantages of the RSEI Model

The influencing factors of ecological environmental quality are complex and diverse. Although the evaluation of a single index has some value, it is difficult to explain the comprehensive effect of multiple factors in the ecological environment [10–12]. The RSEI was constructed from four indicators, greenness, humidity, heat, and dryness, thereby solving the one-sided problem of using a single indicator in the evaluation of ecological environmental quality. It can be seen from Table 2 that the average contribution rate of the four indicators to the first principal component (PC1) reached 89.66%, indicating that the PC1 concentrated most of the characteristics of the four indicators; therefore, the RSEI constructed on the basis of PC1 would be more representative than a single indicator. According to the results in Table 3, the average correlation of the RSEI was the highest (0.497), also showing that the RSEI was more suitable for evaluating the quality of the ecological environment than a single indicator. Therefore, compared with other indices, the RSEI index has the advantages of being comprehensive, objective, and efficient in assessing the changing state of the ecological environmental quality, as well as being convenient for visualization, spatiotemporal analyses, modeling, and prediction [14,34–36]. However, the four ecological indicators are still not enough in comparison, so more suitable indicators should be found and added to the RSEI model in order to improve it. Although the RSEI cannot fully reflect the ecological environmental quality of the basin, it is the most comprehensive option among the existing ecological indices; accordingly, it is currently the most widely used.

5.2. Advantages of Constructing the RSEI Model Based on the GEE Platform

Traditional RSEI modeling uses a local computer to download, process, and analyze data. In contrast, the GEE platform can directly use the global Landsat surface reflection data recorded since 1984 without downloading images. Thus, it can not only achieve a real-time update of the image but also removes the need for the complicated preprocessing of remote sensing images [37]. At the same time, the massive remote sensing data for large-scale areas can be quickly processed and analyzed online using Google's powerful servers [38]. These advantages of the GEE platform ensure that the RSEI of any region in the YRB can be obtained in a timely manner. From the modeling results in this paper, not only was the load of each index extracted by the GEE platform found to be consistent with the actual situation (greenness and humidity were positive effects, heat and dryness were negative effects) but the contribution rates of each index to PC1 also exceeded 85% (Table 2). This shows that the RSEI constructed using the GEE platform accurately reflects the ecological environmental quality of the YRB, laying a foundation for accurately analyzing the spatiotemporal change of ecological environmental quality.

Compared with traditional RSEI modeling, the use of the GEE platform allows researchers to focus more on the research purpose itself, rather than on repetitive technical work [39]. The GEE platform provides many built-in codes and functions, such as the cloud mask code, image synthesis code, principal component analysis code, ridge regression function, and linear regression function [40]. These built-in codes and functions ensure that researchers can quickly and accurately determine changes in the regional RSEI, as well as make predictions regarding the future ecological environmental quality of the region. In this paper, a principal component analysis was not applied using other software, such as MATLAB or SPSS, but using the GEE platform for direct coding, which greatly increased the efficiency of the study. In addition, this paper used ridge regression to calculate the RSEI change trend and obtain the corresponding significance, which was significantly more efficient than the traditional one-variable linear regression and F-test [9,23]. Through the application of methods including a trend change analysis and significance analysis, the change law of the ecological environment in the YRB can be explored. Through visualizations, the main change areas can be intuitively found, the reasons can be analyzed, and targeted opinions can be put forward. Therefore, compared with traditional RSEI modeling, the GEE platform is more suitable as a computing platform for large-scale ecological environmental quality monitoring and evaluation. The GEE platform has broad application prospects in the implementation of ecological environmental protection and high-quality development strategies in the YRB in this country.

5.3. Reasons for the Spatiotemporal Change in Ecological Environmental Quality

In recent decades, due to climate change, the ecological environment of the YRB has also changed. In areas in which disasters have occurred, the environment has also been effectively improved [29]. The YRB covers a vast area, where the topography and climate among regions vary greatly, resulting in different ecological environments. The southeastern part of the YRB is mostly a semi-humid climate, which is suitable for vegetation growth. The northwestern part of the YRB is located in arid and semi-arid areas of China, with harsh climatic conditions, widely distributed deserts, and desertified grasslands, which are not suitable for vegetation growth [28,29].

According to the analysis in this paper, the areas with bad (I) and poor (II) ecological environmental quality levels in the YRB were concentrated in the upper and middle reaches of the Yellow River (Figure 6), representing the aggregation of areas with poor ecological environmental quality (Figure 12). The main reason for this is that the natural environment in the region itself is poor, being subject to long-term unreasonable human activities [4]. Therefore, this region has a fragile ecological environment and is suffering from serious soil erosion [41]. However, the upper and middle reaches of the Yellow River were also the regions where the ecological environment quality has most rapidly improved in the past 30 years (1990–2020) (Figures 9 and 10). This is due to the country's long-term active

implementation of ecological and soil erosion control projects—such as the Conversion of Farmland to Forests and Grasses Project, which began in 1999; the Loess Plateau Check Dam Pilot Project, which began in 2003; and the Agricultural Comprehensive Development Soil and Water Conservation Project, which began in 2005—resulting in a significant recovery of the ecological environment in the upper and middle reaches of the Yellow River [3,42]. Restoring the ecological environment is not a short-term task, and while we are improving the ecological policies, we should continue to maintain or increase investment in the area's ecological and environmental protection. The quality of the ecological environment in the lower reaches of the YRB was relatively stable and mainly moderate (III) and good (IV) (Figure 6), with the main reason for this being that downstream rainwater is abundant and the temperature is moderate, which make suitable conditions for vegetation growth and restoration [28]. However, the ecological environmental quality in some areas declined (Figure 9). This was mainly due to the population increase and social and economic development resulting from urban expansion. It is necessary to have both "gold and silver mountains" and "lucid waters and lush mountains", which are both key points and difficulties that cannot be ignored in the future economic development of the lower YRB.

According to the comprehensive analysis of this paper, the overall ecological environmental quality of the YRB improved significantly from 1990 to 2020 (Figure 4), but the improvement was not linear; it was obviously divided into two stages of rapid (1990–2000) and slow (2000–2020) improvements (Figure 5). The main reason for this is that the state has increased its investment in the ecological environment management of the YRB since the 1990s, and the number of nature reserves has also correspondingly and significantly increased [43,44]. As a result, the areas of the YRB with poor ecological quality rapidly improved (Table 4). However, since 2000, the improvement of the ecological environmental quality of the YRB has slowed down. Although the ecological environmental quality of the entire YRB has shown an overall improvement in the past 30 years, the ecological environment in some areas, mainly some large national economic development zones, has shown a worsening trend (Figures 9 and 10). The main reason for the deterioration is that after 2000, human economic activities in these areas caused a great disturbance to the ecological environment, resulting in the degradation of areas in the YRB that previously had good ecological quality (Table 5). With the overall improvement of the ecological environmental quality of the YRB, the regional ecological environmental quality tended to remain at the same level. The area of cold spot aggregation has gradually decreased, while the significance of area corresponding to hot spot aggregation has also gradually decreased (Figure 12). According to the Hurst sustainability analysis, the ecological environmental quality of the YRB will continue to show a trend of continuous improvement for a period of time in the future (Figure 11). The ecological protection and governance of the YRB have been strengthened, and the living environment of the people has also improved. As the economy undergoes development, the ecological environment must also be protected. Therefore, the provinces and cities in the YRB, as well as the country in general, should attach importance to the coordination of the economic development and ecological environmental protection, which is also a requirement to achieve ecological protection and high-quality development.

6. Conclusions

In this study, an analysis of ecological environmental quality changes in the YRB from 1990 to 2020 was carried out using the RSEI. Using spatiotemporal change data, trend analyses, and aggregation states, the ecological and index changes in the YRB region were analyzed, resulting in the following findings.

Because we used the Google Earth Engine (GEE) platform for the modeling and analysis of the remote-sensing-based ecological index (RSEI), the spatiotemporal changes in the ecological environmental quality of the YRB could be obtained in a timely and accurate manner. This has broad application prospects for strategies aimed at high-quality development. Exploring the correlation of other indicators and optimizing the RSEI model

constitute directions for future research. In terms of the ecological environmental quality, the distribution in the YRB exhibited an obvious regional aggregation, with poor-quality areas concentrated in the upper and middle reaches of the Yellow River. However, these are also the areas in the YRB where the ecological environment quality most rapidly improved from 1990 to 2020. The effects from the implementation of China's ecological projects were most obvious in this region, and we should continue to maintain or increase investment in ecological environmental protection in this region. At the same time, the follow-up research should be more detailed, determining the main influencing factors and providing a clear direction for ecological environmental governance. In summary, over the past 30 years, the ecological environmental quality of the YRB has generally improved, and this improvement can be divided into two periods characterized by rapid improvement (1990–2000) and slow improvement (2000–2020). In the future, the quality of the ecological environment in the YRB will be sustainably improved. The improvement of the ecological environment is the most effective means to prevent and control disasters in the YRB. However, the ecological environment of some national key economic development zones is deteriorating; therefore, the provinces and cities in the YRB, as well as the country in general, should focus their attention on the ecological protection and high-quality development of economic development zones, which are of great importance.

Author Contributions: Conceptualization, Z.Y. and J.T.; methodology, Z.Y. and W.S.; validation, Z.Y., J.T. and W.S.; formal analysis, Z.Y. and J.W.; investigation, Z.Y. and J.L.; resources, Z.Y., J.T. and W.L.; data curation, Z.Y. and W.S.; writing—original draft preparation, Z.Y.; writing—review and editing, Z.Y. and R.G.; visualization, Z.Y.; supervision, J.T.; project administration, J.T. and W.L; funding acquisition, J.T. and W.L. All authors have read and agreed to the published version of the manuscript.

Funding: This research was funded by the National Natural Science Foundation of China (31960330) and the Ningxia Natural Science Foundation of China (2020AAC03112).

Institutional Review Board Statement: Not applicable.

Informed Consent Statement: Not applicable.

Data Availability Statement: The data presented in this study are available on reasonable request from the corresponding author.

Conflicts of Interest: The authors declare no conflict of interest.

References

1. Xi, J.P. Speech at the Symposium on Ecological Protection and High-quality Development in the Yellow River Basin. *Struggle* **2019**, *20*, 4–10.
2. Han, P.; Wang, Y.X.; Li, D.F. Spatial and Temporal Variations of Baseflow and Its Responses to Soil and Water Conservation in Hekouzhen-Longmen Section in the Middle Reaches of the Yellow River. *J. Basic Sci. Eng.* **2020**, *28*, 505–521.
3. Zhao, A.Z.; Liu, X.F.; Zhu, X.F.; Pan, Y.Z.; Chen, S.C. Spatiotemporal analyses and associated driving forces of vegetation coverage change in the Loess Plateau. *China Environ. Sci.* **2016**, *36*, 1568–1578.
4. Hung, J.T.; Cao, Y.P.; Qin, F. Analysis of Eco-environment Quality Based on Land Use/Cover Change in the Yellow River Basin. *J. Henan Univ. Nat. Sci.* **2020**, *50*, 127–138.
5. Fang, C.L. Basic rules and key paths for high-quality development of the new urbanization in China. *Geogr. Res.* **2019**, *38*, 13–22.
6. Wang, Y.; Zhao, Y.H.; Wu, J.S. Dynamic monitoring of long time series of ecological quality in urban agglomerations using Google Earth Engine cloud computing: A case study of the Guangdong-Hong Kong-Macao Greater Bay Area, China. *Acta. Ecol. Sin.* **2020**, *40*, 8461–8473.
7. Mateo, G.G.; Gómez, C.L.; Amorós, J.; Muñoz, J.; Camps, G. Multitemporal cloud masking in the Google earth engine. *Remote Sens.* **2018**, *10*, 1079. [CrossRef]
8. Rai, P.K. Forest and land use mapping using Remote Sensing and Geographical Information System: A case study on model system. *Environ. Skept. Crit.* **2013**, *2*, 97–107.
9. Chen, W.; Huang, H.; Tian, Y.C.; Du, Y.Y. Monitoring and Assessment of the Eco-Environment Quality in the Sanjiangyuan Region based on Google Earth Engine. *J. Geo-Inf. Sci.* **2019**, *21*, 1382–1391.
10. Ivits, E.; Buchanan, G.; Olsvig, W.L.; Cherlet, M. European farmland bird distribution explained by remotely sensed phenological indices. *Environ. Model. Assess.* **2011**, *16*, 385. [CrossRef]

11. Coutts, A.M.; Harris, R.J.; Phan, T.; Livesley, S.J.; Williams, N.S.G.; Tapper, N.J. Thermal infrared remote sensing of urban heat: Hotspots, vegetation, and an assessment of techniques for use in urban planning. *Remote Sens. Environ.* **2016**, *186*, 637–651.
12. Guo, W.H.; Wu, L.M.; Zuo, X.Q.; Fang, G. Water body extraction of Huainan city based on TM images. *Geotechnical. Investig.* **2018**, *46*, 64–67.
13. Wang, C.S.; Duan, Y.X.; Zhang, R. Spatial pattern evolution of cities and influencing factors in the historical Yellow River Basing. *J. Nat. Resour.* **2021**, *36*, 69–86.
14. Xu, H.Q. A remote sensing urban ecological index and its application. *Acta. Ecol. Sin.* **2013**, *33*, 7853–7862.
15. Zhu, D.Y.; Chen, T.; Zhen, N.; Niu, R.Q. Monitoring the effects of open-pit mining on the eco-environment using a moving window-based remote sensing ecological index. *Environ. Sci. Pollut. Res.* **2020**, *27*, 15716–15728.
16. Hang, X.; Li, Y.C.; Luo, X.C.; Xu, M.; Han, X.Z. Assessing the ecological quality of Nanjing during its urbanization process by using satellite, meteorological, and socioeconomic data. *J. Meteorol. Res.* **2020**, *34*, 280–293.
17. Yang, J.Y.; Wu, T.; Pan, X.Y.; Du, H.T.; Li, J.L.; Zhang, L.; Men, M.X.; Chen, Y. Ecological quality assessment of Xiongan New Area based on remote sensing ecological index. *Chin. J. Appl. Ecol.* **2019**, *30*, 277–284.
18. Song, H.M.; Xue, L. Dynamic monitoring and analysis of ecological environment in Weinan City, Northwest China based on RSEI model. *Chin. J. Appl. Ecol.* **2016**, *27*, 3913–3919.
19. He, Z.; He, J.P. Remote Sensing on Spatio-temporal Evolution of V egetation Cover in the Yellow River Basin during 1982–2013. *Trans. Chin. Soc. Agr. Mach.* **2017**, *48*, 179–185.
20. Guo, B.B.; Fang, Y.L.; Jin, X.B.; Zhou, Y.K. Monitoring the effects of land consolidation on the ecological environmental quality based on remote sensing: A case study of Chaohu Lake Basin, China. *Land Use Policy* **2020**, *95*, 104569.
21. Shan, W.; Jin, X.B.; Ren, J.; Wang, Y.C.; Xu, Z.G.; Fan, Y.T.; Gu, Z.M.; Hong, C.Q.; Lin, J.H.; Zhou, Y.K. Ecological environment quality assessment based on remote sensing data for land consolidation. *J. Clean. Prod.* **2019**, *239*, 118126. [CrossRef]
22. Liu, P.; Ren, C.Y.; Wang, Z.M.; Zhang, B.; Chen, L. Assessment of the eco-environmental quality in the Nanweng River Nature Reserve, Northeast China by remote sensing. *Chin. J. Appl. Ecol.* **2018**, *29*, 3347–3356.
23. Huang, J.P.; Zhang, G.L.; Yu, H.P.; Wang, S.S.; Guan, X.D.; Ren, Y. Characteristics of climate change in the Yellow River basin during recent 40 years. *J. Hydraul. Eng.* **2020**, *51*, 1048–1058.
24. Xiao, D.Y.; Niu, H.P.; Yan, H.X.; Fan, L.X.; Zhao, S.X. Spatiotemperal evolution of land use pattern in the Yellow River Basin (Henan section) from 1990 to 2018. *Trans. Chin. Soc. Agr. Econ.* **2020**, *36*, 271–281.
25. Gao, J.X.; Wang, Y.C.; Hou, P.; Wan, H.W.; Zhang, W.G. Temporal and spatial variation characteristics of land surface water area in the Yellow River basin in recent 20 years. *J. Hydraul. Eng.* **2020**, *51*, 1157–1164.
26. Wang, M.; Feng, X.Z.; Du, X.L.; Zhao, M.X.; Liang, Q.D. Spatial-temporal Distribution of Air Quality and Its Influencing Factors in the Yellow River Basin. *Total Environ. Prot.* **2019**, *47*, 56–61.
27. Lv, Z.Y.; Mu, J.X. Study on Spatial and Temporal Evolution Feature of Water Quality in Yellow River Basin. *Yellow River* **2017**, *39*, 66–70.
28. Zhao, C.P.; Chen, Y.; Wang, W.G.; Gao, Z.Y. Temporal and Spatial Variation of Extreme Precipitation Indexes of the Yellow River Basin in Recent 50 Years. *Yellow River* **2015**, *37*, 18–22.
29. Fu, J.B. Coordinating Management of the Eco-environmental Systems in the Yellow River Basin. *J. Irrig. Drain.* **2020**, *39*, 130–137.
30. Zhou, L.M.; Wang, S.H. Remote sensing monitoring and evaluation of spatial and temporal changes of ecological environment in Hangjin Banner, Inner Mongolia, China. *Chin. J. Appl. Ecol.* **2020**, *31*, 1999–2006.
31. Yuan, B.; Fu, L.; Zou, Y.; Zhang, S.; Chen, X.; Li, F.; Deng, Z.; Xie, Y. Spatiotemporal change detection of ecological quality and the associated affecting factors in Dongting Lake Basin, based on RSEI. *J. Clean. Prod.* **2021**, *302*, 126995. [CrossRef]
32. Guan, J.Y.; Yao, J.Q.; Li, M.Y.; Zheng, J.H. Assessing the Spatiotemporal Evolution of Anthropogenic Impacts on Remotely Sensed Vegetation Dynamics in Xinjiang, China. *Remote Sens.* **2021**, *13*, 4651. [CrossRef]
33. Zhang, S.Y.; Shao, H.Y.; Li, X.Q.; Xian, W.; Shao, Q.F.; Yin, Z.Q.; Lai, F.; Qi, J.G. Spatiotemporal Dynamics of Ecological Security Pattern of Urban Agglomerations in Yangtze River Delta Based on LUCC Simulation. *Remote Sens.* **2022**, *14*, 296. [CrossRef]
34. Nong, L.P.; Wang, J.L. Dynamic monitoring of ecological environment quality in Kunming based on RSEI model. *Chin. J. Ecol.* **2020**, *39*, 2042–2050.
35. Rukeya, S.; Abuduheni, A.; Li, H.; Nijat, K.; Li, X.H. Dynamic Monitoring and Analysis of Ecological Environment in Fukang City Based on RSEI Model. *Res. Soil Water Conserv.* **2020**, *27*, 283–289.
36. Liu, L.B.; Xiong, K.N.; Ren, X.D. Assessment of Ecological Environment Status in the Longxi-Hongkou National Nature Reserve Based on Remote Sensing Ecological. *J. Ecol. Rural Environ.* **2020**, *36*, 202–210.
37. Gorelick, N.; Hancher, M.; Dixon, M.; Ilyushchenko, S.; Thau, D.; Moore, R. Google Earth Engine: Planetary-scale geospatial analysis for everyone. *Remote Sens. Environ.* **2017**, *202*, 18–27. [CrossRef]
38. Hao, B.F.; Han, X.J.; Ma, M.G.; Liu, Y.T.; Li, S.W. Research Progress on the Application of Google Earth Engine in Geoscience and Environmental Sciences. *Remote Sens. Technol.* **2018**, *33*, 600–611.
39. Guo, Y.Q.; Wang, N.J.; Chu, X.S.; Li, C.; Luo, X.Q.; Feng, H. Analyzing vegetation coverage changes and its reasons on the Loess Plateau based on Google Earth Engine. *China Environ. Sci.* **2019**, *39*, 4804–4811.
40. Yan, K.; Chen, H.M.; Fu, D.J.; Zeng, Y.L.; Dong, J.W.; Li, S.W.; Wu, Q.S.; Li, H.L.; Du, S.Y. Bibliometric visualization analysis related to remote sensing cloud computing platforms. *Natl. Remote Sens.* **2022**, *26*, 310–323.

41. Guo, S.; Pei, Y.Q.; Hu, S.; Yang, D.D.; Qiu, H.J.; Cao, M.M. Response of Vegetation Index to Climate Change and Their Relationship with Runoff-Sediment Change in Vellow River Basin. *Bull. Soil Water Conserv.* **2020**, *40*, 2–13.
42. Li, S.D.; Liu, M.C. The Development Process, Current Situation and Prospects of the Conversion of Farmland to Forests and Grasses Project in China. *J. Res. Ecol.* **2022**, *13*, 120–128.
43. Xu, W.Q.; Tang, Q.; Ding, S.Y. Landscape Pattern Dynamic of Xinxiang Yellow River Wetland Bird National Nature Reserve. *Henan Province. Wetl. Sci.* **2016**, *14*, 235–241.
44. Peng, K.F.; Jiang, W.G.; Hou, P.; Sun, C.X.; Zhao, X.; Xiao, R.L. Spatiotemporal variation of vegetation coverage and its affecting factors in the Three-river-source National Park. *Chin. J. Ecol.* **2020**, *39*, 3388–3396.